Article

Not peer-reviewed version

Magmatic Telescoping as a Reflection of the Shift in Geodynamic Circumstances and Patterns of Formation of Gold Ore Manifestations

Inna M. Derbeko *

Posted Date: 3 March 2025

doi: 10.20944/preprints202503.0137.v1

Keywords: Mongol-Okhotsk orogenic belt, late Mesozoic, granitoids, subduction, collision, gold ore manifestations, adakite signature.

 doi:10.20944/preprints202503.0137.v1

Article

Magmatic Telescoping as a Reflection of the Shift in Geodynamic Circumstances and Patterns of Formation of Gold Ore Manifestations

Inna M. Derbeko

Institute of Geology and Nature Management, Russian Academy of Sciences, Far Eastern Branch, Blagovesh-6 chensk, Amur region, Russia derbeko@mail.ru

Abstract: The presented work is the result of the study and the analysis of the distribution of ore manifestations and geochemical fields of gold and magmatic complexes of the Late Mesozoic in the framing of the Eastern flank of the Mongol-Okhotsk orogenic belt. It was found that elevated concentrations of this noble element are noted within the areas of telescoping of rocks of magmatic complexes formed in various geodynamic settings. The main testing ground for studying this problem was the southern framing of the Eastern flank of the Mongol-Okhotsk orogenic belt (Russia). Here, the processes of combining various magmatic stages, is most clearly manifested. The chosen object of study was the intrusive Uskalin massif. The massif is composed of rocks that reflect the following geodynamic events: initial over-subductional (149– 138 Ma), subductional (140– 122 Ma), collisional (119– 97 Ma). The formation of this massif is accompanied by extensive mineralization zones with gold-bearing veins. Therefore, gold contents have been established directly in the granitoids, which exceed the Clarke values by 2.25.

Keywords: Mongol-Okhotsk orogenic belt; late Mesozoic; granitoids; subduction; collision; gold ore manifestations; adakite signature

1. Introduction

The uniqueness of the metallogeny of the Mongol-Okhotsk orogenic belt (MOOB) (Figure 1a) has been known almost since the middle of the 19th century.

 doi:10.20944/preprints202503.0137.v1

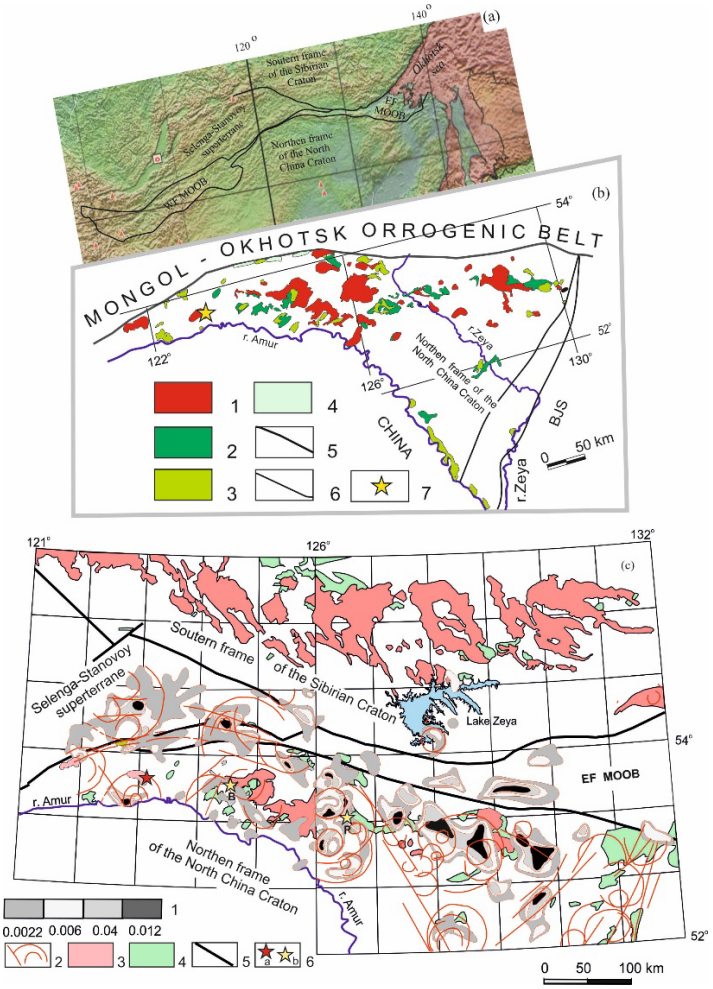

Figure 1. Scheme of the spatial position of the EF MOOB and magmatic complexes in its frame. (a) The position of the MOOB among the regional structures of eastern Asia on the Geological 54 map of the world scale 1:50 000 000 [1]. (b) Spatial distribution of igneous complexes in the southern frame of the EF MOOB: combined bodies of Late Cretaceous granitoids (1); Early Cretaceous volcanic fields of differentiated (2) and bimodal (3) complexes; Cenozoic basalts (4); southern boundary of the EF MOOB (5); regional tectonic boundaries (6); position of the Uskaly massif (7). BJS – Bureya-Jiamusi superterrane. (c) Geochemical gold halos based on lithochemical surveys of dispersion flows at a scale of 1:200,000 [2–4]. Scale of intensity of geochemical gold fields (in g/t) (1). Tectonic elements based on satellite imagery interpretation (2). Granitoids (3) and volcanic fields (4) of the Late Cretaceous. Regional tectonic boundaries (5). Position of the Uskalin massif (6a) and industrial gold ore deposits (6b): Burinda – B, Pokrovka – P.

I.A. Poletika called this region “gold-bearing mountains” [5]. Since that time, not only the development of the riches of this geological object, but also its active study began. By now, it has been established that the MOOB was finally formed by the end of the Early Cretaceous, as a result of the closure of the basin of the same name [6–13]. However, as a result of Cenozoic tectonic events, the belt was divided into two flanks: western and eastern [14,15]. Within the western flank, the geodynamic processes accompanying the closure of the Mongol-Okhotsk Basin (MOB) are significantly obscured by late tectonic and magmatic events. Within the eastern flank, these processes are almost undistorted. Therefore, it is an excellent testing ground for studying the sequence of geological vents and associated ore processes.

The eastern flank of the Mongol-Okhotsk orogenic belt (EFO MOOB) is located entirely in the Amur region (Russia). The Amur region is one of the leading regions of Russia in gold mining. Hundreds of thousands of kilograms of gold have been extracted from its depths [16]. The ore objects identified to date are not large or unique deposits. The relationship between gold mineralization and

 doi:10.20944/preprints202503.0137.v1

late Mesozoic magmatism has been mentioned since the 1960s [17]. In the 2000s, precision data on the geochronology and material composition of igneous rocks in the region were accumulated. This made it possible to study in detail the likelihood of a relationship between late Mesozoic magmatism and gold mineralization. And also to answer the question: the spatial distribution of which igneous complexes should be taken into account in further forecasting of gold ore objects.

The general idea of the features of gold distribution in the frame of the EF MOOB is indicated by their behavior in the bottom sediments of watercourses. To obtain this information, mono-element maps of element concentrations were analyzed based on the materials of primary data of lithochemical surveys along dispersion flows [2–4]. Analysis of the distribution of geochemical fields of gold mineralization showed their confinement to the areas of development of rocks of volcano-plutonic complexes of the late Mesozoic (Figure 1b, c).

The study of the formations of these complexes during mapping was complicated by the fact that several types of rocks are found within one massif. Which led to the identification of up to seven phases of one complex within some massifs. The accumulated statistics on geochronology and material (geochemistry) composition have shown the following: within one massif, rocks of various complexes were formed, accompanying different geodynamic settings. It was established that subduction processes began in the region around 150 Ma, which were accompanied by the formation of volcano plutonic complexes of the adakite series with an age of 149 – 138 Ma [18–20]. The active phase of subduction (140 – 122 Ma) is marked by the formation of rocks of the differentiated calc-alkaline series. About 120 Ma, subduction processes gave way to collisional ones. These events were reflected in the formation of rocks of bimodal complexes (119 – 97 million years) [9,21,22]. The change in geodynamic settings and the formation of magmatic complexes accompanying these geodynamic scenarios are well illustrated by the diagram (Figure 2).

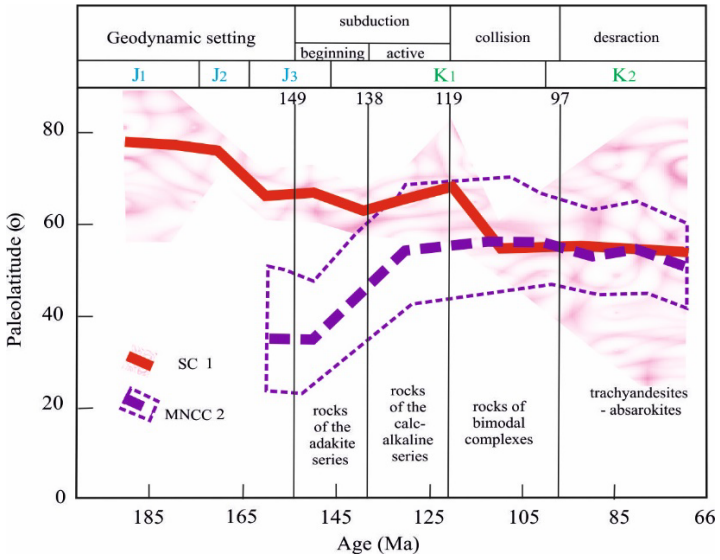

Figure 2. Comparison of paleomagnetic data and the time of formation of igneous complexes within the framework of the EF MOOB. The paleolatitude-time relationship for the reference point 52oN-117oE (MOOB). Average poles averaged within 10-million-year time windows: SC (1) – Siberian craton; MNCC – Mongolian - Chinese Composite Continent. According to [23].

All magmatic processes occurred synchronously in the northern and southern frames. In the north, due to Cenozoic tectonic events, the territory was subjected to intense destruction. Volcanic structures here are significantly eroded. In the south, they are better preserved (Figure 1b).

To solve the problems, the Uskalin massif was chosen as one of the most controversial and complexly constructed objects (Figure3). The massif is located in the upper reaches of the Uskali River - the left bank of the Amur River. The area of the outcrop of this intrusive body is about 60 km2. But it is believed that it represents only the upper part of a large pluton. Determinations of the age of the

 doi:10.20944/preprints202503.0137.v1

rocks are very contradictory. According to [24], they were formed 129.6 ± 0.64 Ma. In the work [25], the formation time of the massif is 145 ± 5 million years. According to the age of formation of this intrusive body, in the first case they were attributed to the Early Cretaceous, and in the second case – to the Late Jurassic. At the same time, all researchers divide the rocks of the Uskalin massif into several phases. In the structure of the massif, granosyenite porphyry, granosyenite, and subalkaline granites are distinguished. The authors [24,25] attributed these rocks to formations of the 1st phase. Subalkaline granites, making up the southwestern part of the massif, are attributed to the 2nd phase. Some of the subalkaline granite porphyry and granite porphyry were identified in local areas of the marginal zones of the intrusion. In the work of [25] these rocks belong to the endocontact facies. In the work of [24] they are described as apical areas. As a result, both authors believe that the Uskalin massif is composed of a single two-phase complex. And the rocks of this complex were formed in an intraplate setting, synchronously with normal alkalinity granitoids and A-type granites. We have studied the southeastern part of the Uskalin massif: petrographic profile d2010 – 2010-6 (Figure 3).

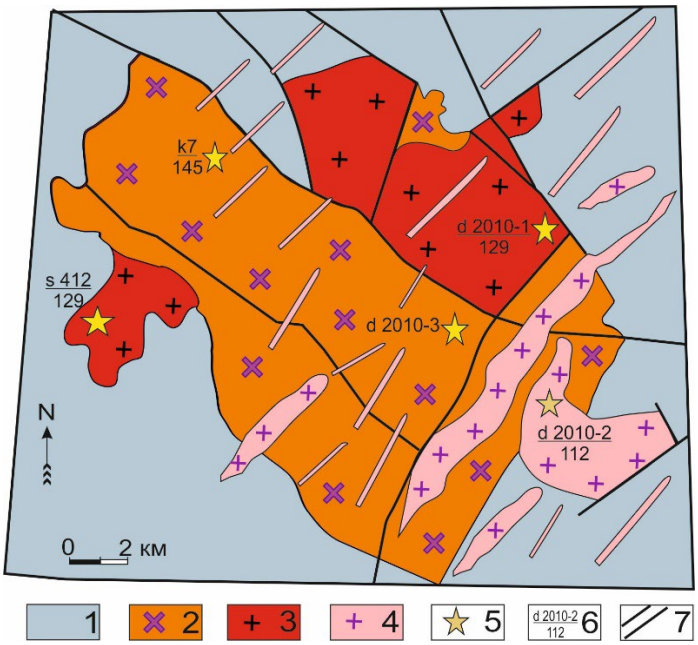

Figure 3. Scheme of the geological structure of the Uskalin massif according to data [[24,25]; the author]. Terrigenous formations of the Middle – Late Jurassic (1); granitoids of the adakite series (2); differentiated calcareous-alkaline (3); bimodal (4). sampling sites (5). Sample numbers: s [24], k [25], d [author's details] (numerator), age of rock (denominator) (6). Tectonic contacts (7).

2. Materials and Methods

Mineralogical and petrographic characteristics of 12 representative samples of granitoids were studied using an Axio Scope A1 polarizing microscope. Determination of the contents of rock-forming elements and some trace elements (V, Cr, Co, Ni, Cu, Zn, Rb, Sr, Y, Nb, Zr, Ba) in granitoids was performed by the X-ray fluorescence method at the Institute of Geology and Nature Management, Far Eastern Branch of the Russian Academy of Sciences (Blagoveshchensk, Russia) on a Pioneer 4S X-ray spectrometer. Concentrations of trace elements by the ICP-MS method were carried out at the A.P. Vinogradov Institute of Geochemistry, Siberian Branch of the Russian Academy of Sciences (Irkutsk, Russia) on a NexION 300D ICP mass spectrometer. The following microelements were determined by the ICP-MS method: Ga, Ge, Rb, Cs, Sr, Ba, Pb, La, Ce, Pr, Nd, Sm, Eu, Gd, Tb, Dy, Ho, Er, Tm, Yb, Lu, Y, Th, U, Zr, Hf, Nb, Ta, Sc.

Zircon grains for U-Pb geochronological studies were isolated in the mineralogical laboratory of the Institute of Geology and Nature Management FEB RAS (Blagoveshchensk, Russia) using heavy liquids. The studied zircons from the Uskalin massif granites (sample d2010-1, d2010-2) are

 doi:10.20944/preprints202503.0137.v1

represented by short- and long-prismatic transparent and semi-transparent crystals of a slightly yellowish color of a subhedral or euhedral shape. In the cathodoluminescence image, they are characterized by concentric and sectorial growth zoning.

U-Pb geochronological studies on the differentiated series granitoids (sample d2010–1) and rocks that were assigned by predecessors to the endocontact facies (sample d2010–2) were carried out at the Geospectrum Collective Use Center of the Geological Institute SB RAS (Ulan-Ude, Russia) using an Element XR single-collector magnetic sector mass spectrometer with inductively coupled plasma (Termo Scientific). The mass spectrometer is equipped with a UP-213 laser ablation device (New Wave Research). A detailed description of the analytical procedures is presented in the publication [26]. The obtained results were processed using the Glitter [27] and Isoplot v. 3.6 [28] programs.

3. Results

3.1. Petrographic Features and Age of Granitoids of the Uskalin Massif

The structure of the Uskalin massif includes syenites, granosyenites, subalkaline granites and granite porphyries, normal series granite porphyries, granodiorite porphyries, quartz diorite porphyrites, and granites. All rocks (except granites) are characterized by porphyry structures.

The main mass of syenites and granosyenites is made up of feldspars, quartz, and amphibole, blue-green to brownish in the center of the grains. Porphyry segregations are formed by microcline-perthite, plagioclase (No. 23–27), and quartz. Among the accessory minerals, sphene predominates (up to 2%); zircon, apatite, and an ore mineral are present (Figure 4a).

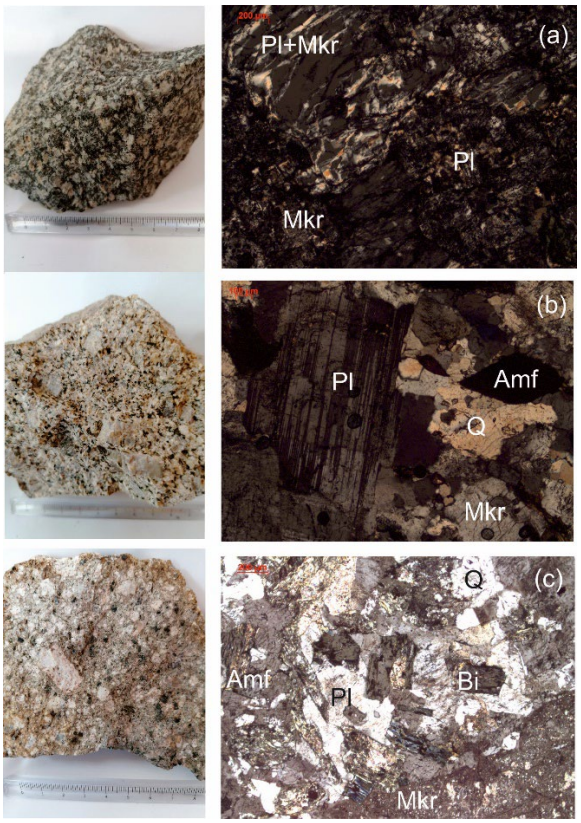

Figure 4. Photomacrographs end photomicrographs (cross-polarized light) for rocks of the Uskalin massiv. (a) granosienite (Sample d2010–3); (b) subalkaline granite (Sample d2010–1); (c) quartz diorite porphyrite (Sample d2010–2). Q – quartz, Pl – plagioclase, Amp – amphibole, Bi – biotite, Mkr – K-Feldspar.

The groundmass in subalkaline granites is represented by quartz, plagioclase (No. 25–28), orthoclase, greenish-brown biotite and blue-green amphibole. Porphyries are formed by microcline

 doi:10.20944/preprints202503.0137.v1

and quartz. Accessory minerals: zircon, sphene, apatite, magnetite, hematite. Subalkaline granite porphyries differ from subalkaline granites only in the structure of the groundmass. They develop a crown structure: small quartz grains are overgrown with plagioclase. Granite porphyries are characterized by a fine-grained groundmass. It is represented by quartz, feldspars, brown biotite. Porphyry segregations are formed by plagioclase (No. 26–33), quartz, brown biotite, and potassium feldspar. Accessory minerals: sphene, apatite, zircon, ore mineral (Figure 4 b). Granodiorite porphyrites are similar in composition to granite porphyries, but rare grains of green amphibole appear in them.

Quartz diorite porphyrites contain plagioclase No. 33–40, green amphibole, brownish-brown biotite, potassium spar, quartz. Sometimes relics of volcanic glass are preserved. Glass is intensively replaced by secondary minerals (Figure 4 c).

Holocrystalline rocks are rare. They are represented by granites with a hypidiomorphic-granular structure. They are composed of quartz, plagioclase No. 26–28, microcline, orange-brown biotite. Accessory minerals: zircon, sphene, ore mineral.

Among the secondary formations in all rocks, pelitic matter, chlorite, sericite, calcite, epidote, saussurite predominate.

Jurassic sedimentary rocks enclosing granitoids of the Uskalin massif underwent intensive contact metamorphism. The contour of the intrusion influence on the host rocks sometimes reaches 2 km. Within these limits, new formations of granoblastic quartz aggregates and lepidoblastic rosette–shaped accumulations of finely flaky brown biotite, sericite flakes, sometimes turning into small muscovite leaflets, and in isolated cases, actinolite, were formed in the terrigenous deposits. Xenoliths of terrigenous rocks altered to quartzite, and veinlets of hornfels quartz are noted at the contact with granites. Quartz gold veins have been established in the contact part of the massif in the north [summary according to 25].

Of all the listed varieties of granitoids, quartz diorite-porphyrites are the most clearly mapped. They form small bodies and dikes that break through the rocks of the Uskalin massif and the terrigenous formations enclosing it. The structure of small bodies shows petrographic zoning, typical of the structure of subvolcanic intrusions: a well-crystallized central part gradually passes to less crystalline areas. In this case, the marginal part is represented by andesites. These rocks (sample d2010–2) were selected for age determination (Figure 3). The age of quartz diorite-porphyrites was 112 Ma (Figure 5), which is comparable in time with the stage of collisional events in the region under consideration, when the formation of bimodal complex formations took place over a period of about 20 Ma (Figure 2).

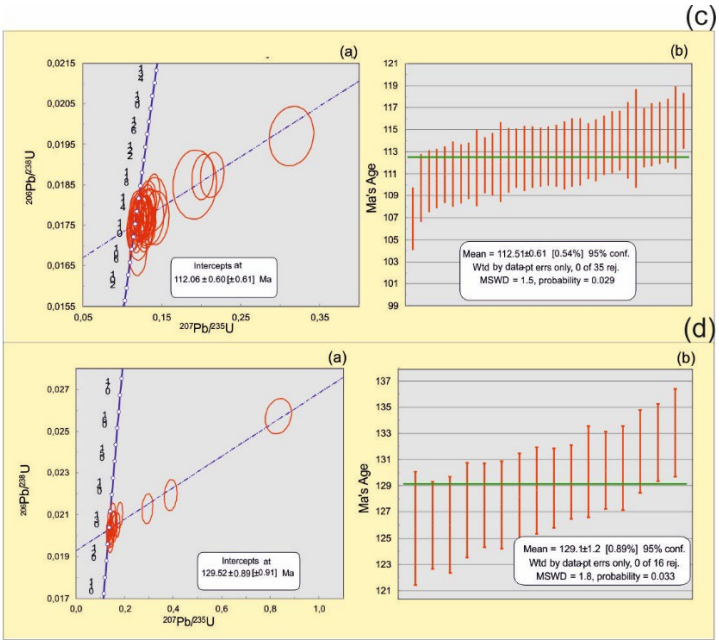

 doi:10.20944/preprints202503.0137.v1

Figure 5. Diagrams with concordia (a) and calculation of the average weighted age (b) for a young population of zircons from quartz diorite porphyrites (sample d2010-2) (c) and subalkaline granites (sample d2010–1) (d) of the Uskalin massif.

The situation is more complicated with mapping plutonic complexes that formed under subduction conditions. At the initial stage of subduction, granitoids of the adakite series are formed, which are often comparable in appearance to subalkaline granitoids of the main stage of subduction. They are also partially superimposed in time of formation (Figure 2) [18,19]. In fact, the main criterion for their identification is the geochemical composition of the rocks. This was analyzed when studying the formations of the Uskalin massif [data were used 23; 24; authors' data].

Geochronological studies by predecessors [24] were carried out for granitoids of the western flank of the massif (Figure 3, s412). The concordant age of the subalkaline granite here was 129.60 ± 0.64 Ma (MSWD = 0.034, probability = 0.85).

We collected a sample from similar subalkaline granites on the eastern flank of the massif (Figure 3, d2010-1). The concordant age of the subalkaline granite here was 129.52 ± 0.89 Ma (Figure 5).

The age of these formations corresponds to the age of rocks formed in suprasubduction conditions (Figure 2). During this time period, the formation of rocks of differentiated calc-alkaline igneous complexes took place, which in their material characteristics are comparable to igneous formations of active continental margin zones [18]. Analysis of the geochemical characteristics of the granitoids of the Uskalin massif showed that its main components are syenites, granosyenites and subalkaline granites of the adakite series. They form the central part of the massif. A distinctive mineralogical feature of these rocks is the presence of blue-green amphibole in the composition. Which is absent in the granitoids of the calc-alkaline series. The age of these subalkaline granites was determined by the K-Ar method for three rock-forming minerals (amphibole, biotite and potassium feldspar) of one sample. It was 145±5 Ma [25]. The age of these formations corresponds to the age of rocks formed under the conditions of the initial stage of subduction (Figure 2) – adakites. This is the time period when the eastern flank of the Mongol-Okhotsk basin, having experienced uplift, begins to subduct, in this case, under the formations of the northern framing of the North China Craton [18,19].

3.2. Geochemical Characteristics of Granitoids of the Uskalin Massif

The description of the geochemical characteristics of rocks of igneous complexes of the Late Mesozoic in the framing of the EF MOOB has already been given in the literature [9,18–22]. In this work, a comparison of the geochemical characteristics of the formations of the Uskalin massif with such characteristics of the Late Cretaceous granitoids of this territory is carried out.

It is known that igneous formations of the adakite series of the southern framing of the EF MOOB belong to the normal or subalkaline series. These are high-potassium products (Na2O + K2O = 7.86–10.92 wt.%) with the Na2O/K2O ratio of 1.25–1.81, magnesian, with the aluminum saturation index = 1.06–0.86, and belong to the I-type formations. Comparable characteristics have been established for the granitoids of the Uskalin massif, where Na2O + K2O = 7.96–9.54, and the Na2O/K2O ratio = 1.08–1.60. The peculiarities of the geochemical composition of these rocks (the characteristics of the Uskalin massif rocks are given in double brackets) include increased concentrations of Sr (670–1110 (762) ppm), Ba (510–1290 (1000) ppm); partially elevated Rb (82–160 (104) ppm), Th (8.4–13.1 (10) ppm) with reduced contents of Nb (4.0–11.0 (5.7) ppm), Ta (0.4–0.6 (0.56) ppm) and with abnormally low concentrations of HREE (in ppm): Tb (0.18–0.22 (0.19)), Dy (0.66–1.45 (0.85)), Ho (0.10–0.22 (0.12)), Er (0.25–0.55 (0.27)), Tm (0.03–0.070.036), Lu (0.02–0.05 (0.03)), as well as Y (3–7 (2.17)) and Yb (0.17–0.42). These characteristics of the material composition are illustrated in (Figure 6a), where they are clearly distinguished from the rocks of the differentiated calc-alkaline complex by their HREE content.

 doi:10.20944/preprints202503.0137.v1

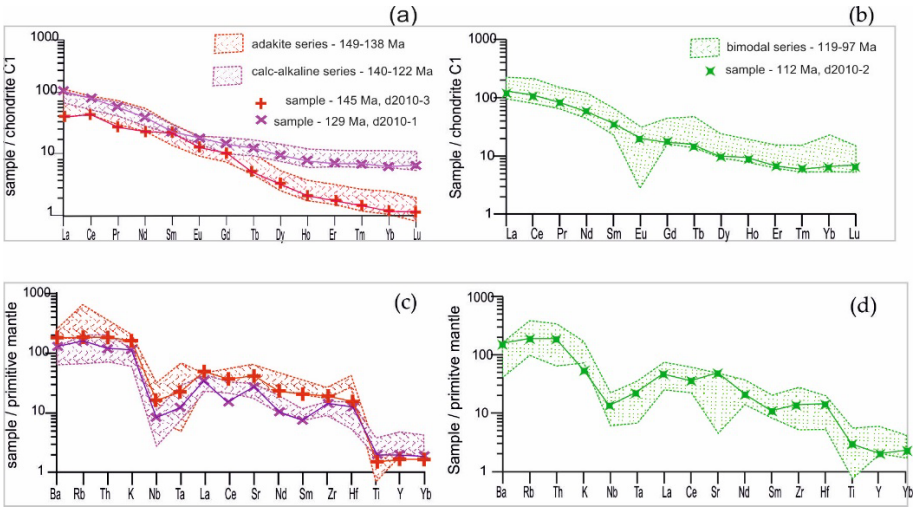

Figure 6. Concentrations of the rare elements in the granitoids of the EF MOOB framing standardized to the composition of Chondrite (a) and primitive mantel (b). Compositions of chondrite C1 and primitive mantel are brought according to the data [29].

These granitoids are also characterized by high Sr/Y and (La/Yb)n ratios, which is confirmed by the location of these values on the classification diagrams (Figure 7).

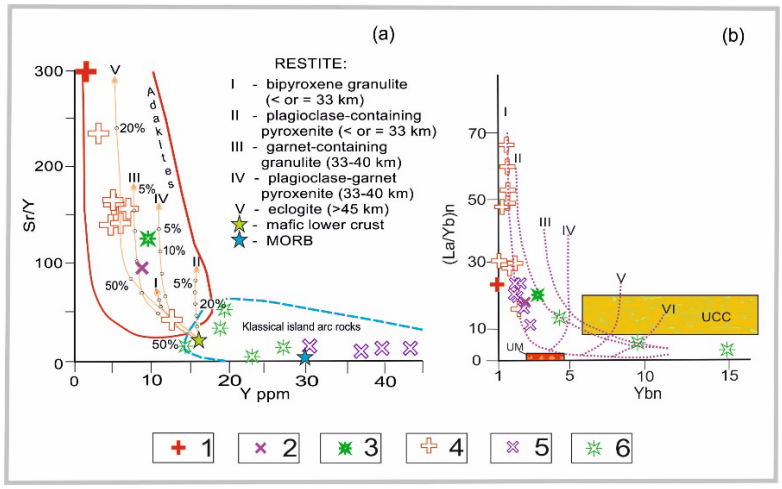

Figure 7. The position of the Uskalin massif granitoids in comparison with the granitoids of the southern framing of the EF MOOB on the diagrams: a) Sr/Y – Y ratios [30]. Partial melting curves were calculated for periodic melting of mafic rocks of the lower crust of the North China Craton from [31]; b) (La/Yb)n – Ybn ratios [30,32,33] with the extracted melting trends of the sources according to [34]: I - quartz eclogites; II - garnet amphibolites; III - amphibolites; IV - garnet-bearing mantle, with a garnet content of 10%; V - garnet-bearing mantle, with a garnet content of 5%; VI – garnet-bearing mantle, with garnet content of 3%; UM – upper mantle; UCC – upper continental crust. Values are normalized to primitive mantle according to [29]. Legend: granosyenites (1), subalkaline granites (2), quartz diorite porphyrites (3) of the Uskalin massif; granitoids of the adakite series (4), calc-alkaline series (5), bimodal series (6) outside the ore bodies.

4. Discussion

The main subduction stage lasted for almost 20 Ma (Figure 2). It was accompanied by the formation of a differentiated calc-alkaline complex [19]. This complex is represented by plutonic (140-128 Ma), hypabyssal (130–124 Ma) and volcanic (128–122 Ma) formations. Granitoids of the Uskalin massif with an age of 129 Ma correspond to the transitional stage between the formation of plutonic

 doi:10.20944/preprints202503.0137.v1

and hypabyssal formations, which are partially combined in time. This is reflected in the composition of the granites of the studied massif: a relatively high Sr content and low Y contents are preserved (Figure 7). Subalkaline granites of the massif belong to the high-potassium calc-alkaline series with a total alkali content of 7.76 wt. % and the ratio Na2O/K2O = 1.1 (in the rocks of the differentiated calc-alkaline complex 0.9–2.2), moderately magnesian. The content of Al2O3 = 15.3 wt.%, which fits into the range of Al2O3 concentration (15.1–16.1 wt.%) in hypabyssal formations. On the chondrite-normalized graph (Figure 6a), the curve of the Uskalin massif granites is located in the lower part of the field for the rocks of the differentiated complex. And according to the ratio with the generalized graph of recalculation of the compositions of the rocks of the differentiated complex to the primitive mantle (Figure 6b), the curve is close to, and for some elements, coincides with such characteristics of adakites. The predominance of LREE over HREE is clearly expressed ((La/Yb)n = 17.4), but these values are closer to the plutonic granitoids of the differentiated complex ((La/Yb)n = 10.4–19.2). Granitoids of the Uskalin massif are significantly depleted in Nb, Ta, Ti, Y, Yb and enriched in Ba, Rb, Th, K (Figure 6 b), which is typical for all formations of the differentiated calc-alkaline series. The subduction stage ended at 122 Ma. And almost immediately (119 Ma), bimodal complexes began to form in the framing of the EF MOOB, which accompanied the collision process (Figure 2). The age of quartz diorite porphyrites is 112 Ma. This is comparable with the age of the stage of collisional events in the region under consideration, which existed in the region for almost 20 million years.

The bimodal volcano plutonic complex in the southern frame is determined by two ranges of SiO2 content: 47–64 and 72–78 wt.% [9,21]. Within the Uskalin massif they are represented by rocks with SiO2 content = 61.55–61.69 wt.% – quartz diorite-porphyrites with an age of 112 Ma. These are moderately low-magnesian, low-titanium (0.57 wt.%) formations with Al2O3 content = 14.77 wt.%. They belong to the low-potassium calc-alkaline series with a total alkali content of 5.96 wt.% and a Na2O/K2O ratio of 3.08. It was found that the rocks of the complex under consideration are enriched in light rare earth elements: (La/Yb)n = 5.5–33.0 (the values of 10–20 prevail), in the diorite-porphyrites of the massif (La/Yb)n = 20.3, the Eu minimum is almost not expressed (Figure 6a), which corresponds to all formations of the complex of average composition (Eu/Eu* = 0.70–0.86). Multielement spectra are characterized by stable positive anomalies of Ba, Rb, Th and negative anomalies of Nb, Ta and Ti. The behavior of Y in these rocks attracts attention. Its content is close to such values in suprasubduction formations. Most likely, the period of formation of the first mode corresponds to the transition of subduction settings to collisional ones, which at the end of the Early Cretaceous (119 – 97 Ma) produced active orogenesis of the EF MOOB. This is confirmed by classical diagrams of tectonic settings (Figure 8a, b). In them, the figureurative points of the diorite porphyrites of the Uskalin massif fall into the field of post- or collisional formation conditions. The rocks of the adakitic and calc-alkaline series are located in the field of island arcs or supra-subduction rocks.

 doi:10.20944/preprints202503.0137.v1

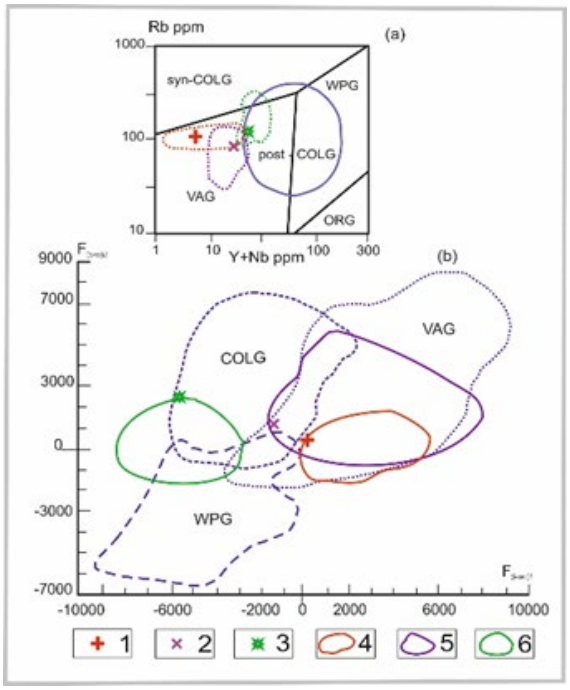

Figure 8. Discrimination diagrams for the formation of the tectonic situations: a) Rb-Y+Nb [35]; b) F(c-w)2/F(i-wc)1 [36]; F(c-w)2 = -752.3* SiO2 – 6537.06* TiO2 – 25.6* Al2O3 - 928.96* Fe2O3* +1928.07* MgO - 464.21* CaO - 1808.19* Na2O - 272.16* K2O + 8675.33* P2O5 + 71073.5; F(i-wc)1 = 2432.42* SiO2 + 7900.33* TiO2 + 2512.12* Al2O3 + 1380.23* FeOt + 2616.55* MgO + 3480.51* CaO + 3045.39* Na2O + 645.91* K2O - 241285.5]. Legend: granosyenites (1), subalkaline granites (2), quartz diorite porphyrites (3) of the Uskalin massif; granitoids of the adakite series (4), calc-alkaline series (5), bimodal series (6) outside the ore bodies.

Our studies have shown that the formation of the Uskalin massif involved igneous complexes of all geodynamic stages of the late Mesozoic, accompanying the evolution of the EF MOOB: adakitic series – differentiated calc-alkaline – bimodal (mode of intermediate - basic composition). At the same time, it has been proven [18] that the rocks of the adakitic series were formed at a depth of 33 - 50 km at a pressure of no more than 13 kbar in a subduction setting at a temperature of up to 1300 °. Melting of the oceanic crust occurred at an orthogonal subduction angle and interaction of the oceanic crust with the overlying mantle and with the continental crust. The heat sources, respectively, were the hot asthenosphere and mechanical characteristics during the subduction of formations of the Mongol-Okhotsk basin. Thus, the steep subsidence of the oceanic plate under the northern rim of the North China Craton probably contributed to the concentration of magmatic sources, which replaced each other in time in accordance with the change in the geodynamic situation, but their areal distribution remained practically unchanged (Figure 9).

 doi:10.20944/preprints202503.0137.v1

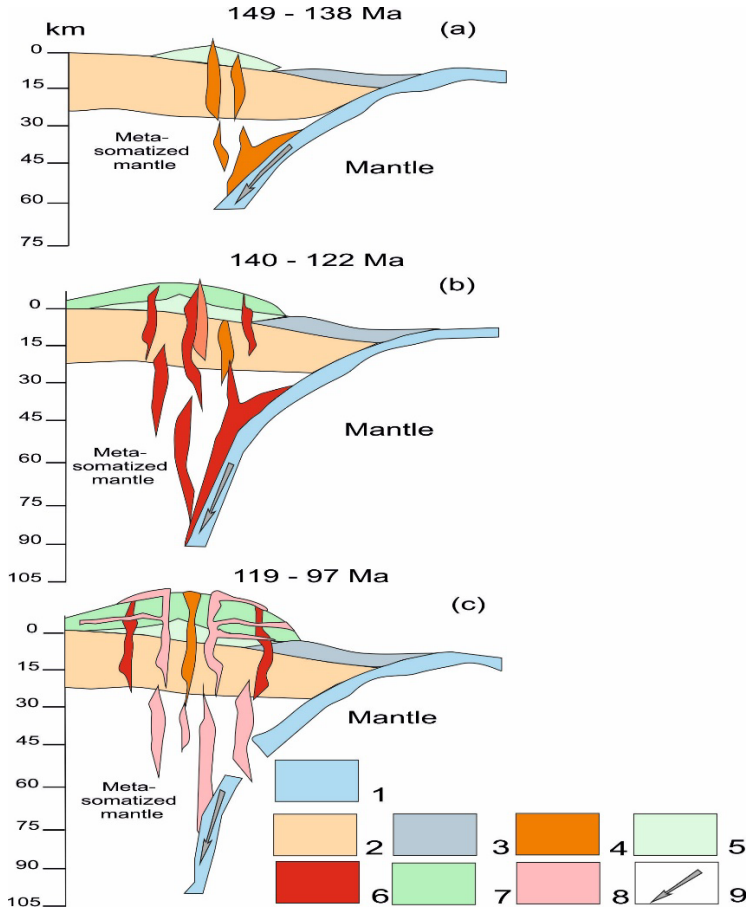

Figure 9. Scheme of the sequence of late Mesozoic igneous complexes formation in the southern framing of the EF MOOB. Oceanic crust (1); continental crust (2); marine sediments (3); adakite melts, plutonic (4) and volcanic (5); calc-alkaline melts, plutonic (6) and volcanic (7); contrasting magmatic melt (8); direction of movement of oceanic crust (9). Stages of igneous complexes formation: a) 149 – 138 Ma, b) 140 – 122 Ma, c) 119 – 97 Ma.

Subduction processes in the region were caused by the convergence of the Siberian and North Chinese cratons. And judging by the magmatic activity, it continued in the range of 150-120 Ma (Figure 2). The subduction scenario changes to the scenario of collisional compression around 120 Ma (119 Ma). It is possible that this stage begins with the breakaway of the subducting plate (Figure 9c). Considering the proximity of the ages of the described magmatic complexes, it can be assumed that the intrusion of the rocks of the bimodal complex occurred in the continental crust heated by subduction processes. This could have caused partial mixing and inheritance of the characteristics of subduction rocks by the formations of the bimodal complex. This is observed in the diorite porphyrites of the bimodal complex of the Uskalin massif. They have elevated Sr/Y values (Figure 7a). The high content of magmatic water formed during subduction contributed to the formation of fluid-rich melts. Getting into the magmatic chamber, they enriched the magmatic material. Fluid enrichment probably occurred unevenly. This is reflected in the distribution of rocks with the "adakite signature" and, accordingly, in the distribution of minerals. A direct relationship is actually established between them. Intrusive bodies are widespread within the territory under consideration, in the structure of which magmatic complexes of different ages are mapped. Gold ore objects have been established mainly where magmatic formations with "adakite signatures" are combined. An example of this is the Burinda massif, located to the east of the Uskalin massif (Figure 1c). According to the results of Ar–Ar isotope dating of granitoids of this massif, its composition is represented by rocks with ages: 142 Ma, 127 – 122 Ma and 117 Ma (Rb-Sr method) [summary on 24]. Rocks of the bimodal complex (117 Ma) are characterized by increased values of Sr/Y. An industrial gold deposit has been discovered within the Burinda massif [37].

 doi:10.20944/preprints202503.0137.v1

The industrial Pokrovka deposit, known in the literature, is 30% composed of granitoids of the adakite series with an age of 139 Ma [37] and rocks of the differentiated complex with an age of 129 Ma [38], which are penetrated by dikes and small bodies of the bimodal complex with an age of 117 Ma [37], 119 and 116 Ma [38]. Directly at the deposit, the formations of the bimodal complex are characterized by Sr/Y ratios of 30-125 with a Y content of 2 to 15 ppm. In quartz diorite porphyrites, similar in composition to the rocks of the Uskalin massif, Sr/Y = 64 with Y = 11 ppm. It should be emphasized that in the rocks of the bimodal complex, mapped outside the gold ore occurrences, the Sr/Y and (La/Yb)n ratios are significantly lower (Figure 7a, b).

The inheritance of "adakite signatures" by rocks can serve as one of the search criteria for gold prospecting in the region. But it should be noted that some characteristics of adakites are not reflected in these formations, such as HREE depletion. If in the adakites of the Uskalin massif the sum of HREE = 3.82 ppm, then in the rocks of the differentiated complex HREE = 14.04 ppm, and in the bimodal ones – HREE = 14.67 ppm.

The watercourses of the Amur Region are characterized by general contamination with placer gold. As a rule, their concentration is noted in the area of the described objects. The identified geochemical anomalies of gold are localized in the fields of development of terrigenous formations intruded by bodies and dikes of rocks of igneous complexes of suprasubduction origin, which in turn are intruded by rocks of the collisional stage of the territory's development (Figure 1c).

The fact that the formation of gold ore objects is associated with the subduction stage of evolution has been mentioned since the middle of the twentieth century. A.H.G. Mitchell and M.S. Garson [39,40] described the concentration of gold-bearing ores in the upper parts of volcanic strata sections in subduction zones on the continental margin. They identified the "Chilean type", i.e., subduction. Currently, the works [41] confirm the connection of gold ore mineralization with subduction scenarios of the evolution of the east coast of China. In the work [42] it was shown that hydrothermal, productive for gold, activity is mainly associated with calc-alkaline magmatism - with rocks of suprasubduction magmatism. The works of E.B. Yeap [43] studied and described gold ore deposits in the subduction zones of Peninsular Malaysia. Similar gold ore objects were established in the Tethys Himalayan belt. The authors [44] believe that gold is associated with subduction processes, which were replaced by collisional ones. The same opinion is shared by [45].

A similar situation is observed in the evolution of ore formation within the Uskalin massif. Hydrothermal productive activity for gold is mainly associated with supra-subduction magmatism. The intrusion of rocks of a later bimodal complex in a collisional setting contributes to the redistribution of metal and an increase in its concentration. Analysis of the geological situation of the southern framing of the EF MOOB showed that areas where gold mineralization is widely manifested are characterized by the presence of telescoped magmatism. At the same time, increased productivity for gold is associated with rocks that are marked by "adakite signatures". This fact can be considered one of the signs for the discovery of epithermal gold ore objects.

5. Conclusion

1. The structure of the Uskalin massif includes rocks that accompany all geodynamic stages of the evolution of the EF MOOB: the initial stage of subduction – the main stage of subduction - the collisional stage. The massif is a product of telescoped magmatic events that occurred in the framing of the EF MOOB in the Late Mesozoic.

2. Analysis of the distribution of geochemical gold fields within the EF MOOB framework indicates an increased concentration of this element within the areas of telescoping of rocks of complexes formed in supra-subduction and collisional settings.

3. The introduction of rocks of the bimodal complex at the end of the Early Cretaceous (119 – 97 Ma) in a collisional setting contributed to the redistribution of metals that were present in a dispersed or diffuse state in supra-subduction formations. Which contributed to their further increased concentration.

 doi:10.20944/preprints202503.0137.v1

4. Such a sequence is noted within those objects where the rocks of the bimodal complex are marked by the "adakite signature". This fact can be considered one of the search criteria for the discovery of epithermal gold ore objects.

Funding: The study was carried out in accordance with the research plan of the Institute of Geology and Nature Management of the Far Eastern Branch of the Russian Academy of Sciences and with partial financial support from the Russian Foundation for Basic Research (grant No. 13-05-12043-ofi-m). The main part of the study was carried out without attracting external funding.

Acknowledgments: Acknowledgments: The author thanks the staff of the Center for Collective Use "Geospectrum" of the Geological Institute of the Siberian Branch of the Russian Academy of Sciences (Ulan-Ude, Russia) for conducting analytical research and the geologists of "Amurgeologiya" LLC for assistance in field work.

Conflicts of Interest: The authors declare no conflict of interest.

References

1. Bouysse, Ph. Geological map of the World, scale 1:50 000 000, 2009, Available from: http://www.ccgm.org.
2. Sokolov, S.V. Structures of anomalous geochemical fields and mineralization forecast. Nauka: St. Petersburg, Russia, 1998; pp. 131.
3. Derbeko, I.M.; Vyunov, D.L. Distribution of gold and silver mineralization in the territory of the Amur region (Russia) according to geochemical prospecting data and its role in geodynamic reconstructions. In Book Gold of Siberia and the Far East. Buryat Scientific Center SB RAS: Ulan-Ude, Russia, 2004; pp. 69-71.
4. Derbeko, I.M.; Vyunov, D.L.; Bortnikov, N.S. The role of interaction of plume and plate tectonics mechanisms in the formation of gold-silver mineralization of the Upper Amur region (Russia) in the Late Mesozoic. Geology and mineral resources of Siberia. FSUE "SNIIGGiMS": Novosibirsk, Russia, 2014; 3(1), 14-17.
5. Poletika, I.A. General properties of gold deposits. Mining J. 1866, 1-10. (In Russian).
6. Kravchinsky, V.A.; Cogné, J.-P.; Harbert, W.P.; Kuzmin, M.I. Evolution of the Mongol-Okhotsk Ocean as constrained by new palaeomagnetic data from the Mongol-Okhotsk suture zone, Siberia. Geophys. J. Inter. 2002, 148, 34–57. doi:10.1046/j.1365-246x.2002.01557.x.
7. Xiao, W.J.; Kusky, T. Geodynamic processes and metallogenesis of the Central Asian and related orogenic belts: Introduction. Gondwana Res. 2009, 16, 167–169.
8. Metelkin, D.V.; Vernikovsky, V.A.; Kazansky, A.Y.; Wingate, M.T.D. Late Mesozoic tectonics of Central Asia based on paleomagnetic evidence. Gondwana Research 2010, 18, 400–419. doi:10.1016/j.gr.2009.12.008
9. Derbeko, I.M. Bimodal volcano-plutonic complexes in the frames of Eastern member of Mongol-Okhotsk orogenic belt, as a proof of the time of final closure of Mongol-Okhotsk basin. In Book Up-dates in volcanology - A Comprehensive Approach to Volcanological Problems, Francesco Stoppa; InTech: Rijeka, Croatia, 2012; Chapter 5, 99-124.
10. Shevchenko, B.F.; Popeko, L.I.; Didenko, A.N. Tectonics and evolution of the lithosphere of the eastern fragment of the MongolOkhotsk orogenic belt. Geodyn. end Tectonoph. 2014., 5(3), 667–682. http://doi:10.5800/GT2014530148
11. Van der Voo, R.; van Hinsbergen, D.J.J.; Domeier, M.; Spakman, W.; Torsvik, T.H. Latest Jurassic–earliest Cretaceous closure of the Mongol-Okhotsk Ocean: A paleomagnetic and seismological-tomographic analysis. Geol. Soc. of America Spec. Pap. 2015, 513, 589–606. doi:10.1130/2015.2513(19)
12. Ren, Q.; Wu, H.; Zhao, H. Further paleomagnetic results from the ~ 155 Ma Tiaojishan Formation, Yanshan Belt, North China, and their implications for the tectonic evolution of the Mongol-Okhotsk suture. Gondwana Res. 2016, 35 180–191. https://doi: 10.1016/j.gr.2015.05.002
13. Ren, Q.; Zhang, S.; Wu, Y.; Yang, T.; Gao, Y.; Turbold, S.; Zhao, H.; Wu, H.; Li, H.; Fu, H.; Xu, B.; Zhang, J.; Tomurtogoo, O. New late Jurassic to early Cretaceous paleomagnetic results from North China and southern Mongolia and their implications for the evolution of the Mongol-Okhotsk suture. J. of Geophysical Res. Solid Earth 2018, 123(12), 10,370–10,398. https://doi.org/10.1029/2018JB016703

 doi:10.20944/preprints202503.0137.v1

14. Derbeko, I.; Kichanova, V. Post-Mesozoic Evolution of the Eastern Flank of the Mongol–Okhotsk Orogenic Belt. Advances in Geophysics, Tectonics and Petroleum Geosciences 2021., CAJG 2019. Springer, Cham, 4, 577-581. https://doi.org/10.1007/978-3-030-73026-0_129
15. Derbeko, I. The Influence of an Interdependent Structures on the Post-Mesozoic Evolution of the Eastern Flank of the Mongol-Okhotsk Orogenic Belt. Intern. J. of Geosc. 2022., 13(6), ttps://doi.org/10.4236/ijg.2022.136025
16. Melnikov V.D.; Melnikov A.V.; Kovtanyuk G.P. Gold placers of the Amur region. 2006, pp. 295.
17. Vetluzhskikh, V.G. Regularities of placement, conditions of formation and prospects for discovery of gold placers in the south of the Aldan Shield and in the Stanovoy folded region. Abstract of a PhD dissertation. Far Eastern Scientific Center of the USSR Academy of Sciences, Vladivostok, Russia, 1972.
18. Derbeko, I.M.; Chugaev, A.V. Late Mesozoic adakite granites of the southern frame of the eastern flank of the Mongol-Okhotsk orogenic belt: material composition and geodynamic conditions of formation. Geodyn. end Tectonoph. 2020, 11(3), 474–490. doi:10.5800/GT-2020-11-3-0487
19. Derbeko, I.M. Late Mesozoic Granitoid Magmatism in the Evolution of the Eastern Flank of the Mongol-Okhotsk Orogenic Belt (Russia). Minerals 2022, 12(11), 1374. https://doi.org/10.3390/min12111374
20. Derbeko, I. Late Mesozoic Adakite Granites in the Northern Framing of the Eastern Flank of the Mongol–Okhotsk Orogenic Belt. Geochem. Intern. 2023, 61(1), 62–74. https://doi.10.1134/S0016702923010020
21. Derbeko, I.M., Ponomarchuk, V.A., Vyunov, D.L., Kozyrev S.K. Bimodal post-collision volcano-plutonic complex in the southern rim of the eastern flank of the Mongol-Okhotsk orogenic belt. In Book: Proceedings of the 24-th IAGS, D.R. Lentz, K.G. Thorne, K.-L. Beal; Canada, 2009; pp. 143--46.
22. Derbeko, I.M.; Vyunov, D.L.; Kozyrev, S.K.; Ponomarchuk, V.A. Conditions for the formation of a bimodal volcano-plutonic complex, within the southern margin on the eastern flank of the Mongol-Okhotsk orogenic belt. In Book Large igneous provinces of Asia, mantle plumes and metallogeny, Novosibirsk, Russia 2009; pp. 73-75.
23. Zhang, K-J.; Yan, L.-L.; Ji, C. Switch of NE Asia from extension to contraction at the mid-Cretaceous: A tale of the Okhotsk oceanic plateau from initiation by the Perm Anomaly to extrusion in the Mongol–Okhotsk ocean? Earth-Science Rev. 2019, 198, 1-12. http://doi.org/10.1016.earscrev.2019.102941
24. Stricha, V.E. U-PB isotope age (shrimp-ii) of granitoids of a magdagachinsky complex of the Umlekano-Ogodzhinsky vulkano-plutonic zone. Bull. of Amur State Univer., Russia 2016, 75, 73 – 74.
25. Kozyrev, S.K.; Volkova, Y.R.; Ignatenko, N.N. State map of the Russian Federation-scale 1: 200 000. Ed. VE Chepygin. Series Zeya. Sheet N-51-XXIII. Explanatory note. Moscow branch of FSBI "VSEGEI": Moscow, Russia, 2016.
26. Khubanov, V.B.; Buyantuev, M.D.; Tsygankov, A.A. U-Pb isotope dating of zircons from PZ-MZ igneous complexes of Transbaikalia by magnetic sector mass spectrometry with laser sampling: procedure for determination and comparison with SHRIMP data. Geol. and Geoph. 2016, 57(1), 241–258.
27. Griffin, W.L.; Powell, W.J.; Pearson, N.J.; O'Reilly, S.Y. GLITTER: data reduction software for laser ablation ICP-MS. In Book Laser ablation ICP-MS in the Earth sciences: current practices and outstanding issues. Mineralogical association of Canada short course series; P.J. Sylvester; Canada 2008, 40, 204–207.
28. Ludwig, K.R. Isoplot 3.6: Berkeley Geochronology Center. Spec. Publ., 2008, 4 77.
29. Sun, S-s.; McDonough, W.F. Chemical and isotopic systematics of oceanic basalts: implications for mantle composition and processes. In Book Magmatism in the Ocean Basins; A.D. Sounders, M.J. Norry; The Geol. Soc. Spec. Public.: London, England, 1989, Volume 42, pp. 313–345. http://dx.doi.org/10.1144/GSL.SP.1989.042.01.19
30. Defant, M.J.; Drummond, M.S. Derivations of some modern are magmas by melting of young subducted lithosphere. Nature 1990, 347, 662-665. http://dx.doi.org/10.1038/347662a0
31. Ma, Q.; Zheng, J.P.; Xu, Y.G.; Griffin, W.L.; Zhang, R.S. Are continental "adakites" derived from thickened or foundered lower crust? Earth. Planet. Sci. Lett. 2015, 419, 125-133. http://dx.doi.org/10.1016/j.epsl.2015.02.036
32. Martin, H. The mechanisms of petrogenesis of the Archaean continental crust - comparison with modern processes, Lithos 1993, 46, 373-388.

 doi:10.20944/preprints202503.0137.v1

33. Martin, H. Adakitic magmas: modern analogues of Archaean granitoids, Lithos 1999, 46(3), 411-429. https://doi.org/10.1016/S0024-4937(98)00076-0
34. Barbarian B. Granitoids: main petrogenetic classifications in relation to origin and tectonic setting. Geol. J. 1990, 25, 227-238.
35. Pearce, J. Sources and settings of granitic rocks. Episodes 1996, 24, 956-983.
36. Velicoslavinsky, S.D. Geochemical typification of acid magmatic rocks of leading geodynamical situations. Petrology 2003, 26(2), 363-380,
37. Eirish, I.V. Metallogeny of golg of Priamurye (Amur Region, Russia), V.A. Stepanov; Dalnauka: Vladiostok, Russia, 2002; pp. 97 - 121.
38. Sorokin, A.A.; Kadashnikova, A.Y.; Ponomarchuk, A.V.; Travin, A.V.; Ponomarchuk, V.A. Age and genesis of the Pokrovskoye gold-silver deposit (Russian Far East). Geol. and Geoph. 2021, 62(1), 165-176.
39. Mitchell, A.H.G.; Garson, M.S. Mineralization of plate boundaries. Minerals. Sci. Engng. 1976. 8, 129-169.
40. Mitchell, A.H.G.; Garson, M.S. Mineral Deposits and Global Tectonic Settings (Academic Press Geology Series). Published by Academic Press Inc: London, UK, 1981.
41. Browne, P.R.L.; Hedenquist, J.W.; Allis, R.G. Epitherminal gold mineralization; Belousov V.I.; Geothermal Research Centre: Wellington, New Zealand. 1988, pp. 169.
42. Qiu, K.-F.; Deng J.; Laflamme C.; Long, Z.-Y.; Wana R.-Q.; Moynier; F.; Yu H.-C.; Zhang, J.-Y.; Ding Z.-J.; Goldfarb R. Giant Mesozoic gold ores derived from subducted oceanic slab and overlying sediments. Geoch. et Cosmoch. Acta 2023, 343, 133–141. https://doi.org/10.1016/j.gca.2023.01.002
43. Yeap, E.B. Tin and gold mineralizations in Peninsular Malaysia and their relationships to the tectonic development. J. of Southeast Asian Earth Scienc. 1993, 8, 1–4, 329-348.
44. Zheng, W.; Liu, B.; McKinley, J.M.; Cooper, M.R.; Wang, L. Geology and geochemistry-based metallogenic exploration model for the eastern Tethys Himalayan metallogenic belt, Tibet. J. of Geoch. Explor. 2021, 224, 106743. https://doi.org/10.1016/j.gexplo.2021.106743
45. Zheng, Y.; Mao, J.; Chen, Y.; Sun, W.N.P.; Yang, X. Hydrothermal ore deposits in collisional orogens. Science Bull. 2019. www.elsevier.com/locate//scib